

## An Electrochemical Approach toward the Metastable Type II Clathrate Germanium Allotrope

Bodo Böhme\*

Cite This: *Inorg. Chem.* 2020, 59, 11920–11924

Read Online

ACCESS |

Metrics & More

Article Recommendations

Supporting Information

**ABSTRACT:** By using an anodic conversion process at 280 °C, the type II clathrates  $\text{Na}_{1.7(6)}\text{Ge}_{136}$  and  $\text{Na}_{23.0(5)}\text{Ge}_{136}$  were obtained from  $\text{Na}_{12}\text{Ge}_{17}$  as the starting material. An alkali-metal iodide molten-salt electrolyte complied with the reaction conditions, allowing for the formation of microcrystalline products. Characterization by powder X-ray diffraction, scanning electron microscopy, and energy-dispersive X-ray spectroscopy also revealed  $\text{Na}_4\text{Ge}_{13}$  as an intermediate and  $\alpha\text{-Ge}$  and  $\text{Cs}_{8-x}\text{Ge}_{136}$  as byproducts, with the latter likely resulting from cation exchange between the starting material and electrolyte. Taking such minor side reactions and a small contribution of material without suitable electrical contact into account, anodic conversion of  $\text{Na}_{12}\text{Ge}_{17}$  to  $\text{Na}_{1.7}\text{Ge}_{136}$  proved to proceed without parasitic processes and to comprise the material bulk. The hitherto existing preparation method for  $\text{Na}_{x \rightarrow 0}\text{Ge}_{136}$  by gas–solid oxidation of  $\text{Na}_{12}\text{Ge}_{17}$  has thus been translated into a scalable high-temperature electrochemical approach with enhanced tools for reaction control, promising access to pure  $\text{Ge}(cF136)$  and  $\text{Na}_{24}\text{Ge}_{136}$  after process optimization.

Semiconductor materials continue to be of major interest for, e.g., more efficient solar cells, battery electrode materials, or optoelectronic devices. This coincides with fundamental-science investigations on related intermetallic phases<sup>1–3</sup> and on metastable allotropes of semiconductor elements or their derivative compounds,<sup>4–12</sup> particularly also those with clathrate types of structure.<sup>13–24</sup> One prominent representative is the germanium allotrope  $\text{Ge}(cF136)$ <sup>16,17</sup> (Figure 1), which has been closely linked to the development of redox-preparation methods for metastable allotropes and intermetallic phases. First identified as an oxidation product of  $\text{Na}_{12}\text{Ge}_{17}$ <sup>25</sup> after reaction with an ionic liquid,<sup>16</sup> it has become available in the laboratory scale by gas–solid redox approaches<sup>26,27</sup> and, more recently, by an elaborate thermal degradation technique.<sup>19</sup> However, more easily scalable preparation methods, at best precluding the formation of byproducts by an improved reaction control, are desirable if application as an electronic material<sup>19,28</sup> is further pursued.

Herein, a high-temperature electrochemical redox approach toward  $\text{Ge}(cF136)$  and the derivative  $\text{Na}_{24-\delta}\text{Ge}_{136}$  clathrate is introduced. Again,  $\text{Na}_{12}\text{Ge}_{17}$  was the starting material. In the course of bulk anodic conversion at 280 °C, it depleted in Na and transformed into a microcrystalline type II clathrate material. Depending on gross conversion,  $\text{Na}_{24-\delta}\text{Ge}_{136}$  and  $\text{Na}_{x \rightarrow 0}\text{Ge}_{136}$  were found to be the main crystalline products. With a sufficiently low melting point, a mixture of LiI, NaI, and CsI was applied as a molten-salt electrolyte. Aluminum metal served as the cathode material, acting as a selective acceptor for  $\text{Li}^+$  ions (Figure S1). The formation of elemental alkali metals at the cathode with possible adverse effects<sup>29–31</sup> was not observed. The overall cell reaction is given in eq 1.

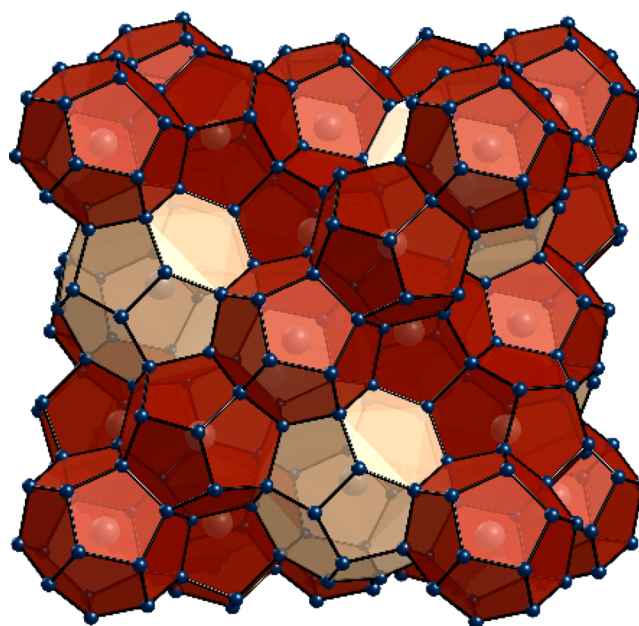
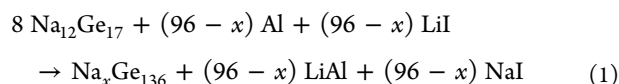
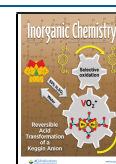


**Figure 1.** Type II clathrate crystal structure<sup>13</sup> of  $\text{Na}_x\text{Ge}_{136}$ . Covalently four-bonded Ge atoms (blue spheres) arrange into a framework, creating pentagonal dodecahedral  $5^{12}$  (red) and hexakaidecahedral  $5^{12}6^4$  (pale red) cages, which are practically completely filled by Na atoms (gray spheres) for  $\text{Na}_{24-\delta}\text{Ge}_{136}$  and completely empty for the allotrope  $\text{Ge}(cF136)$ .

Received: June 17, 2020

Published: August 24, 2020



To control the potential of the  $\text{Na}_{12}\text{Ge}_{17}$  anode, diamond-type germanium ( $\alpha\text{-Ge}$ , *cF8*) was used as a pseudoreference electrode. The potential of metastable  $\text{Ge}$  (*cF136*) as the target of an exhaustive oxidation of  $\text{Na}_{12}\text{Ge}_{17}$  was therefore assumed close to 0 V versus  $\alpha\text{-Ge}$ . To keep the reference potential stable and unaffected by the cell reaction within the applied three-electrode setup (Figure 2), an electrolyte melt saturated in CsI

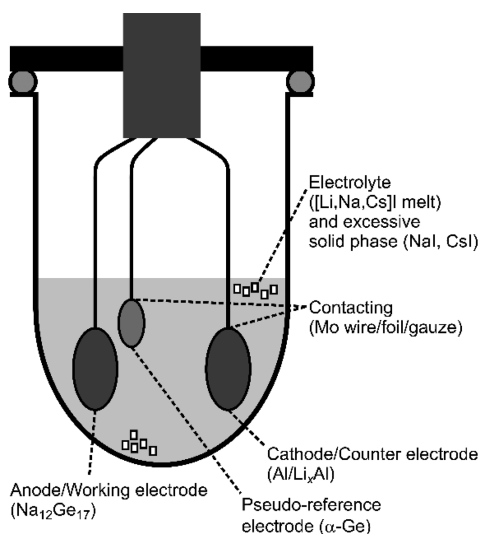


**Figure 2.** Setup principle for anodic conversion of  $\text{Na}_{12}\text{Ge}_{17}$  to  $\text{Na}_{x\rightarrow 0}\text{Ge}_{136}$  or  $\text{Na}_{24\rightarrow 6}\text{Ge}_{136}$  at 280 °C.

and NaI was chosen. The nominal LiI–NaI–CsI composition (mass ratio 3.62:1:5.35) consequently yielded three phases at 280 °C:<sup>32</sup> the electrolyte melt and solid NaI and CsI. At constant temperature, liberation of  $\text{Na}^+$  from the anode and consumption of  $\text{Li}^+$  at the cathode thus result in the further precipitation of NaI only (eq 1). Molybdenum served as an inert contacting material applicable in halide melts.<sup>33,34</sup> More experimental details are provided in ref 35 and the Supporting Information.

Gradual anodic conversion of the  $\text{Na}_{12}\text{Ge}_{17}$  working-electrode material (Figure S2) was controlled by a chronoamperometric approach: The working-electrode potential was increased stepwise toward the target potential of 0 V (vs  $\alpha\text{-Ge}$ ), starting from the initial open-circuit potential (−0.65 V), and gross conversion was monitored by the transferred charge (Figure 3). Anodic conversion was allowed to proceed freely at the respective adjusted potential, until falling below a minimum current (conversion rate). Subsequently, the next potential was adjusted, if applicable (see the Supporting Information). In a remarkable analogy to chemical gas–solid oxidation of  $\text{Na}_{12}\text{Ge}_{17}$  to  $\text{Ge}$  (*cF136*) at 280 °C,<sup>26,27</sup> anodic conversion proceeded for almost 10 days to completion (Figure 3). After 20% gross conversion, the target potential of 0 V had to be adjusted. Afterward, a steady reaction was indicated by an almost constant current (slope of the transferred-charge curve) for the next 3 days. At about 80% gross conversion, the current (conversion rate) distinctly decreased, but a steady further reaction at a lower rate was observed for a further 6 days. Such behavior might result from the disappearance of a particular phase, the kinetically less hindered Na depletion of which had been rate-determining by then. Possibly, the lowered rate indicates exclusive Na depletion of the type II clathrate  $\text{Na}_x\text{Ge}_{136}$ . More detailed studies are needed here.

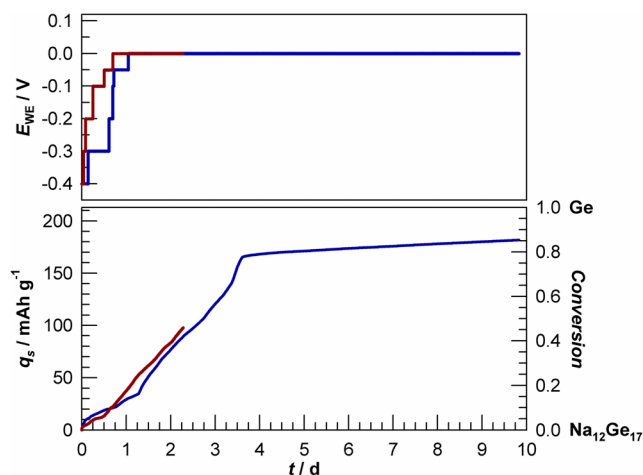


**Figure 3.** Anodic conversion of  $\text{Na}_{12}\text{Ge}_{17}$  by means of chronoamperometry at 280 °C: Chronological development of the adjusted working-electrode potential  $E_{\text{WE}}$  (vs  $\alpha\text{-Ge}$ ) of the  $\text{Na}_{12}\text{Ge}_{17}$  anode (top) and the transferred charge  $q_s$  normalized to the set-in  $\text{Na}_{12}\text{Ge}_{17}$  mass, with corresponding gross conversion of  $\text{Na}_{12}\text{Ge}_{17}$  to elemental Ge [ $\alpha\text{-Ge}$  or  $\text{Ge}$  (*cF136*) cannot be distinguished here] as the assumed product (bottom). Measurements for the two independent experiments are represented by blue and red curves.

The phases obtained after complete anodic conversion of  $\text{Na}_{12}\text{Ge}_{17}$  to 0 V versus  $\alpha\text{-Ge}$  were elucidated by investigating the working-electrode material after cooling and washing with alcohol and water. The final product was separated with a yield of about 67 mass %, as calculated for complete conversion to  $\text{Ge}$  (*cF136*). According to Rietveld refinement<sup>36</sup> of the powder X-ray diffraction (PXRD) data (Figure 4), it consisted mainly of

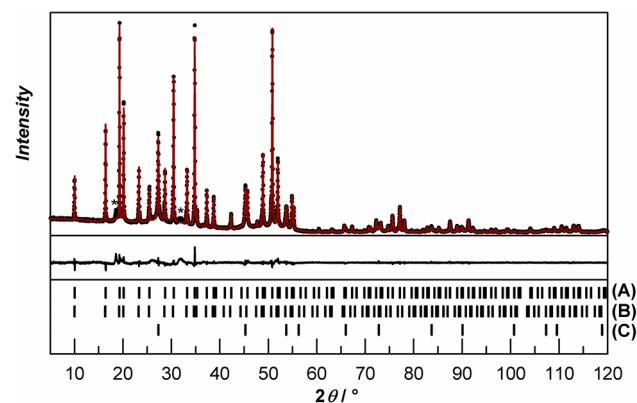


**Figure 4.** PXRD pattern (Stoe Stadi MP diffractometer, Cu  $K\alpha_1$  radiation,  $\lambda = 1.540598$  Å, and zero-background sample holder) of the washed product from complete anodic conversion of  $\text{Na}_{12}\text{Ge}_{17}$  for 10 days at 280 °C, showing the experimental data (black dots) and calculated pattern after Rietveld refinement (red curve), with their difference plotted below. Ticks in the lower part mark the positions of the Bragg reflections for  $\text{Na}_{1.7(6)}\text{Ge}_{136}$  (A),  $\text{Cs}_{6.4(16)}\text{Ge}_{136}$  (B), and  $\alpha\text{-Ge}$  (C), and asterisks mark reflections of an unidentified phase.

a crystalline type II clathrate phase (about 70 mass %) at the composition  $\text{Na}_{1.7(6)}\text{Ge}_{136}$ . Consistent with the low Na content assigned, the lattice parameter of 15.2272(3) Å determined versus the internal  $\text{LaB}_6$  standard<sup>37</sup> was only slightly larger than that observed for  $\text{Ge}$  (*cF136*) from gas–solid oxidation<sup>27</sup> and close to that of  $\text{Na}_x\text{Ge}_{136}$  ( $x \approx 4.5$ ) obtained by thermal degradation<sup>19</sup> (Table S1).  $\alpha\text{-Ge}$  (18 mass %) and a second type

II clathrate (12 mass %) were detected as byproducts. For the latter, Rietveld refinement indicated empty dodecahedral cages but large scattering power within the hexakaidecahedral cages. When Cs filling was assumed,  $\text{Cs}_{6.4(16)}\text{Ge}_{136}$  was refined. The result was corroborated by the lattice parameter of  $a = 15.301(1)$  Å, possibly hinting at a composition somewhat poorer in Cs than  $\text{Cs}_8\text{Ge}_{136}$  with  $a = 15.329$  Å.<sup>38</sup> However, Na + Cs mixed occupancy might likewise explain the observed scattering power in the hexakaidecahedral cages of that phase, and more elaborate studies are needed to elucidate that issue.

Investigations by scanning electron microscopy (SEM) and electron-dispersive X-ray spectroscopy (EDXS) adequately confirmed the presence of Cs, particularly in individual particles (see the Supporting Information), and estimated a suitable overall content in the specimen of about 2 mass %. Likewise, in agreement with PXRD, Na was hardly detectable in the sample, while Ge was the main component (about 98 mass %). The presence of a Cs-containing clathrate actually indicates partial cation exchange of the working-electrode material with the electrolyte. However, former experiments have shown that Cs atoms do not refill the empty clathrate cages of  $\text{Ge}(cF136)$  at 280 °C, although such a reaction is known for Na, K, and Rb.<sup>27</sup> Moreover, thermal degradation of  $\text{Na}_{16}\text{Cs}_8\text{Ge}_{136}$  stops at  $\text{Cs}_8\text{Ge}_{136}$ <sup>38</sup> and Cs atoms do not escape. Cation exchange with an already existing crystalline Na-containing clathrate seems thus unlikely. Rather, it should occur with the salt-like  $\text{Na}_{12}\text{Ge}_{17}$ <sup>25</sup> starting material or an intermediate. To avoid Cs contamination, methodical optimization might comprise electrolytes such as  $\text{NaAlCl}_4$ , provided that they are inert toward the redox-sensitive starting material.<sup>39</sup> Such an investigation might also disprove the possibility that the residual electron density assigned to 1.7(6) Na atoms in the main phase might actually originate from, e.g., 0.34(1) nonremovable Cs atoms.

An additional PXRD investigation of the clathrate product, by adding  $\text{LaB}_6$  as an internal intensity standard, revealed practically complete crystallinity (see the Supporting Information). The product, therefore, does not contain noncrystalline contaminants in significant amounts. This investigation also confirmed that the unidentified crystalline phase (Figure 4), not being accounted for in Rietveld refinement, may be present with a low mass fraction only, in agreement with the weak reflections observed. In conclusion, the phase and sample compositions revealed by PXRD are in line with SEM/EDXS and with gross conversion of 85% based on the transferred charge (Figure 3). Because the refinement results suggest nearly complete conversion to elemental Ge ( $\text{Na}_{x \rightarrow 0}\text{Ge}_{136}$  and  $\alpha\text{-Ge}$ ), only about 10–15 mass % of the  $\text{Na}_{12}\text{Ge}_{17}$  starting material should not have reacted. Actually, the presence of unreacted material was indicated by gas formation upon washing with alcohol and water, and the aqueous solution was markedly basic ( $\text{pH} \approx 11$ ). The anodic conversion is, nevertheless, evidenced to comprise the bulk of the  $\text{Na}_{12}\text{Ge}_{17}$  starting material, while providing a high selectivity for  $\text{Na}_{x \rightarrow 0}\text{Ge}_{136}$ .

To identify intermediates involved in the anodic conversion process of  $\text{Na}_{12}\text{Ge}_{17}$ , a reaction was stopped at about 50% gross conversion (Figure 3). After washing, a type II clathrate of composition  $\text{Na}_{23.0(5)}\text{Ge}_{136}$  was revealed as the main crystalline phase (56 mass %). Different from  $\text{Na}_{1.7(6)}\text{Ge}_{136}$ , the clathrate cages are practically completely Na-filled in that case. The lattice parameter of  $a = 15.4412(7)$  Å agreed with the Na-rich  $\text{Na}_x\text{Ge}_{136}$  compositions reported earlier.<sup>13,27</sup> As minor products,  $\text{Na}_{x \rightarrow 0}\text{Ge}_{136}$  (23 mass %) and the Cs-containing phase (5 mass

%) were detected, again, with equal composition and lattice parameters (see the Supporting Information). This finding indicates that the potential of 0 V versus  $\alpha\text{-Ge}$  determines the final products of anodic conversion.  $\alpha\text{-Ge}$  (9 mass %) was revealed as a byproduct, again. However, different from the completed anodic conversion, also  $\text{Na}_4\text{Ge}_{13}$ <sup>40,41</sup> was detected (8 mass %). Not being present after the completed reaction,  $\text{Na}_4\text{Ge}_{13}$  and  $\text{Na}_{24-\delta}\text{Ge}_{136}$  consequently occur as intermediates of anodic conversion of  $\text{Na}_{12}\text{Ge}_{17}$  toward elemental Ge, which is in line with reports on thermal degradation of  $\text{Na}_4\text{Ge}_4$ <sup>42</sup> and chemical gas–solid oxidation of  $\text{Na}_{12}\text{Ge}_{17}$ .<sup>43</sup> However, so far  $\text{Na}_{24-\delta}\text{Ge}_{136}$  has never been conserved as the main product. Thermal degradation of epitaxially grown  $\text{Na}_4\text{Ge}_4$  at suitably low temperature has provided access only to thin films of that phase.<sup>44</sup> Higher temperatures and rapid conversion applied to prepare bulk products favored the formation of the more temperature-stable  $\text{Na}_4\text{Ge}_{13}$ , which, however, rapidly degraded to  $\alpha\text{-Ge}$  rather than to  $\text{Na}_{24-\delta}\text{Ge}_{136}$ .<sup>42</sup> On the other hand, although gas–solid oxidation of  $\text{Na}_{12}\text{Ge}_{17}$  at 280 °C may lead to small amounts of  $\text{Na}_{24-\delta}\text{Ge}_{136}$  after short reaction times,<sup>43</sup> the method does not provide sufficient control of the redox potential to hinder Na depletion of the clathrate during bulk conversion. Once emptied, refilling of the  $\text{Ge}(cF136)$  cages to  $\text{Na}_{24-\delta}\text{Ge}_{136}$  by using Na vapor was similarly hard to control.<sup>27</sup> Anodic conversion of  $\text{Na}_{12}\text{Ge}_{17}$  is, therefore, the first preparation method with a realistic prospect to access the completely Na-filled type-II germanium clathrate in bulk. By adjustment to a slightly lower anode potential presumed to target  $\text{Na}_{24}\text{Ge}_{136}$ , even the unintended formation of  $\alpha\text{-Ge}$ , usually occurring with only few mass percent, but besides X-ray amorphous products in the gas–solid oxidation products,<sup>26,27</sup> might be suppressed. From hitherto experience in gas–solid oxidation,<sup>26,27,43</sup>  $\alpha\text{-Ge}$  is indicative of reactions bypassing the formation of  $\text{Na}_{24-\delta}\text{Ge}_{136}$ , which is required to yield  $\text{Na}_{x \rightarrow 0}\text{Ge}_{136}$  with pure  $\text{Ge}(cF136)$  as the end point of the subsequent Na depletion. Optimization of the yield and selectivity seems thus feasible.

Coming along with both potential control and in situ traceability for the redox reaction and leading to a well-crystalline bulk material because of applicability at suitably high temperatures, the anodic conversion approach in inorganic salt melts provides a substantial further development of the redox-preparation method. For preparative usage, it may overcome the restrictions of recent related room-temperature approaches for kinetically favorable topotactical reactions.<sup>8,9</sup> Anodic conversion complements electrochemical preparation methods for crystalline intermetallic compounds, alloys, or semiconductor materials, which so far have been successful mostly for cathodic processes.<sup>2,45–48</sup> It promises not only to promote the fabrication of  $\text{Ge}(cF136)$  and other crystalline metastable semiconductor allotropes such as  $\text{Si}(cF136)$ <sup>14,15</sup> or  $\text{Ge}(oP32)$ <sup>4</sup> but also to make a variety of intermetallic phases of the Na–Ge and comparable systems preparatively accessible.

## ■ ASSOCIATED CONTENT

### SI Supporting Information

The Supporting Information is available free of charge at <https://pubs.acs.org/doi/10.1021/acs.inorgchem.0c01796>.

Details on chemicals and the preparation of  $\text{Na}_{12}\text{Ge}_{17}$ , on the manufacturing of electrodes and cell assembly, on the chronoamperometric procedure, on PXRD investigations for phase analysis and crystallinity studies, on the structure refinement and refinement results, and on the

SEM/EDXS results and crystallographic data with the results of multiphase Rietveld refinement for the main phases  $\text{Na}_{1.7(6)}\text{Ge}_{136}$  and  $\text{Na}_{23.0(5)}\text{Ge}_{136}$  (PDF)

## AUTHOR INFORMATION

### Corresponding Author

Bodo Böhme – Department Chemical Metals Science, Max Planck Institute for Chemical Physics of Solids (MPI CPFS), 01187 Dresden, Germany; [orcid.org/0000-0003-3102-1130](https://orcid.org/0000-0003-3102-1130); Email: [bodo.boehme@cpfs.mpg.de](mailto:bodo.boehme@cpfs.mpg.de)

Complete contact information is available at: <https://pubs.acs.org/10.1021/acs.inorgchem.0c01796>

### Notes

The author declares no competing financial interest.

## ACKNOWLEDGMENTS

I am grateful for support by my colleagues at MPI CPFS. Particular thanks go to R. Cardoso, S. Hückmann, Yu. Prots, and H. Borrmann for recording of PXRD data, to P. Scheppan and U. Burkhardt for SEM/EDX investigations, and to M. Baitinger and Yu. Grin for helpful discussion of the manuscript. Thanks also go to V. Laurinavichyute, O. Drozhzhin, and E. Antipov for methodical discussion. Support by Deutsche Forschungsgemeinschaft within the Priority Program SPP 1708 “Material Synthesis Near Room Temperature” is gratefully acknowledged.

## REFERENCES

- (1) Pöttgen, R.; Dinges, T.; Eckert, H.; Sreeraj, P.; Wiemhöfer, H.-D. Lithium-Transition Metal-Tetrelides – Structure and Lithium Mobility. *Z. Phys. Chem.* **2010**, *224*, 1475–1504.
- (2) Tambornino, F.; Sappl, J.; Pultar, F.; Cong, T. M.; Hübner, S.; Gifftthaler, T.; Hoch, C. Electrocrystallization: A Synthetic Method for Intermetallic Phases with Polar Metal–Metal Bonding. *Inorg. Chem.* **2016**, *55*, 11551–11559.
- (3) Huggins, R. A. Lithium Alloy Electrodes. In *Handbook of Battery Materials*; Besenhard, J. O., Ed.; Wiley-VCH: Weinheim, Germany, 1999; pp 359–381.
- (4) Tang, Z.; Litvinchuk, A. P.; Gooch, M.; Guloy, A. M. Narrow Gap Semiconducting Germanium Allotrope from the Oxidation of a Layered Zintl Phase in Ionic Liquids. *J. Am. Chem. Soc.* **2018**, *140*, 6785–6788.
- (5) McMillan, P. F.; Gryko, J.; Bull, G.; Arledge, R.; Kenyon, A. J.; Cressey, B. A. Amorphous and nanocrystalline luminescent Si and Ge obtained via a solid-state chemical metathesis synthesis route. *J. Solid State Chem.* **2005**, *178*, 937–949.
- (6) Neiner, D.; Chiu, H. W.; Kauzlarich, S. M. Low-Temperature Solution Route to Macroscopic Amounts of Hydrogen Terminated Silicon Nanoparticles. *J. Am. Chem. Soc.* **2006**, *128*, 11016–11017.
- (7) Kiefer, F.; Hlukhy, V.; Karttunen, A. J.; Fässler, T. F.; Gold, C.; Scheidt, E.-W.; Scherer, W.; Nylén, J.; Häussermann, U. Synthesis, structure, and electronic properties of 4H-germanium. *J. Mater. Chem.* **2010**, *20*, 1780–1786.
- (8) Scherf, L. M.; Hattendorff, J.; Buchberger, I.; Geier, S.; Gas-teiger, H. A.; Fässler, T. F. Electrochemical synthesis of the allotrope allo-Ge and investigations on its use as an anode material. *J. Mater. Chem. A* **2017**, *5*, 11179–11187.
- (9) Zeilinger, M.; Jantke, L.-A.; Scherf, L. M.; Kiefer, F. J.; Neubüser, G.; Kienle, L.; Karttunen, A. J.; Konar, S.; Häussermann, U.; Fässler, T. F. Alkali Metals Extraction Reactions with the Silicides  $\text{Li}_5\text{Si}_4$  and  $\text{Li}_3\text{NaSi}_6$ : Amorphous Si versus allo-Si. *Chem. Mater.* **2014**, *26*, 6603–6612.
- (10) Armatas, G. S.; Kanatzidis, M. G. Mesostructured germanium with cubic pore symmetry. *Nature* **2006**, *441*, 1122–1125.
- (11) Sun, D.; Riley, A. E.; Cadby, A. J.; Richman, E. K.; Korlann, S. D.; Tolbert, S. H. Hexagonal nanoporous germanium through surfactant-driven self-assembly of Zintl clusters. *Nature* **2006**, *441*, 1126–1130.
- (12) Beekman, M.; Kauzlarich, S. M.; Doherty, L.; Nolas, G. S. Zintl Phases as Reactive Precursors for Synthesis of Novel Silicon and Germanium-Based Materials. *Materials* **2019**, *12*, 1139.
- (13) Cros, C.; Pouchard, M.; Hagenmuller, P. Sur une Nouvelle Famille de Clathrates Minéraux Isotypes des Hydrates de Gaz et de Liquides. Interprétation des Résultats Obtenus. *J. Solid State Chem.* **1970**, *2*, 570–581.
- (14) Gryko, J.; McMillan, P. F.; Marzke, R. F.; Ramachandran, G. K.; Patton, D.; Deb, S. K.; Sankey, O. F. Low-density framework form of crystalline silicon with a wide optical band gap. *Phys. Rev. B: Condens. Matter Mater. Phys.* **2000**, *62*, R7707–R7709.
- (15) Ammar, A.; Cros, C.; Pouchard, M.; Jaussaud, N.; Bassat, J. M.; Villeneuve, G.; Duttine, M.; Ménétrier, M.; Reny, E. On the clathrate form of elemental silicon,  $\text{Si}_{136}$ : preparation and characterisation of  $\text{Na}_x\text{Si}_{136}$  ( $x \rightarrow 0$ ). *Solid State Sci.* **2004**, *6*, 393–400.
- (16) Guloy, A. M.; Ramlau, R.; Tang, Z.; Schnelle, W.; Baitinger, M.; Grin, Yu. A guest-free germanium clathrate. *Nature* **2006**, *443*, 320–323.
- (17) Fässler, T. F. Germanium(*cF136*): A New Crystalline Modification of Germanium with the Porous Clathrate-II Structure. *Angew. Chem., Int. Ed.* **2007**, *46*, 2572–2575.
- (18) Kim, D. Y.; Stefanoski, S.; Kurakevych, O. O.; Strobel, T. A. Synthesis of an open-framework allotrope of silicon. *Nat. Mater.* **2015**, *14*, 169–173.
- (19) Baranowski, L. L.; Krishna, L.; Martinez, A. D.; Raharjo, T.; Stevanovic, V.; Tamboli, A. C.; Toberer, E. S. Synthesis and optical band gaps of alloyed Si–Ge type II clathrates. *J. Mater. Chem. C* **2014**, *2*, 3231–3237.
- (20) Beekman, M.; Baitinger, M.; Borrmann, H.; Schnelle, W.; Meier, K.; Nolas, G. S.; Grin, Yu. Preparation and Crystal Growth of  $\text{Na}_{24}\text{Si}_{136}$ . *J. Am. Chem. Soc.* **2009**, *131*, 9642–9643.
- (21) Böhme, B.; Guloy, A.; Tang, Z.; Schnelle, W.; Burkhardt, U.; Baitinger, M.; Grin, Yu. Oxidation of  $\text{M}_4\text{Si}_4$  ( $\text{M} = \text{Na}, \text{K}$ ) to Clathrates by HCl or  $\text{H}_2\text{O}$ . *J. Am. Chem. Soc.* **2007**, *129*, 5348–5349.
- (22) Böhme, B.; Bobnar, M.; Ormeci, A.; Peters, S.; Schnelle, W.; Baitinger, M.; Grin, Yu. Type-I silicon clathrates containing lithium. *Z. Kristallogr. - Cryst. Mater.* **2017**, *232*, 223–233.
- (23) Langer, T.; Dupke, S.; Trill, H.; Passerini, S.; Eckert, H.; Pöttgen, R.; Winter, M. Electrochemical Lithiation of Silicon Clathrate-II. *J. Electrochem. Soc.* **2012**, *159*, A1318–A1322.
- (24) Böhme, B.; Bonatto Minella, C.; Thoss, F.; Lindemann, I.; Rosenburg, M.; Pistidda, C.; Möller, K. T.; Jensen, T. R.; Giebeler, L.; Baitinger, M.; Gutfleisch, O.; Ehrenberg, H.; Eckert, J.; Grin, Yu.; Schultz, L. B1-Mobilstor: Materials for Sustainable Energy Storage Techniques – Lithium Containing Compounds for Hydrogen and Electrochemical Energy Storage. *Adv. Eng. Mater.* **2014**, *16*, 1189–1195.
- (25) Carrillo-Cabrera, W.; Cardoso Gil, R.; Somer, M.; Persil, Ö.; von Schnering, H. G.  $\text{Na}_{12}\text{Ge}_{17}$ : A Compound with the Zintl Anions  $[\text{Ge}_4]^{4-}$  and  $[\text{Ge}_9]^{4-}$  – Synthesis, Crystal Structure, and Raman Spectrum. *Z. Anorg. Allg. Chem.* **2003**, *629*, 601–608.
- (26) Böhme, B.; Hoffmann, S.; Baitinger, B.; Grin, Yu. Application of n-Dodecyltrimethylammonium Chloride for the Oxidation of Intermetallic Phases. *Z. Naturforsch., B: J. Chem. Sci.* **2011**, *66*, 230–238.
- (27) Böhme, B.; Reibold, M.; Auffermann, G.; Lichte, H.; Baitinger, M.; Grin, Yu. Preparation of anionic clathrate-II  $\text{K}_{24-x}\text{Ge}_{136}$  by filling of  $\text{Ge}(cF136)$ . *Z. Kristallogr. - Cryst. Mater.* **2014**, *229*, 677–686.
- (28) Moriguchi, K.; Munetoh, S.; Shintani, A. First-principles study of  $\text{Si}_{34-x}\text{Ge}_x$  clathrates: Direct wide-gap semiconductors in Si-Ge alloys. *Phys. Rev. B: Condens. Matter Mater. Phys.* **2000**, *62*, 7138–7143.
- (29) Liu, J.; Poignet, J.-C. Measurement of the activity of lithium in dilute solutions in molten lithium chloride between 650 °C – 800 °C. *J. Appl. Electrochem.* **1990**, *20*, 864–867.
- (30) Haarberg, G. M.; Osen, K. S.; Egan, J. J.; Heyer, H.; Freyland, W. Electronic Transport in Molten Salt Rich Na - NaX Solutions ( $X = \text{Br}, \text{I}$ ). *Ber. Bunsenges. Phys. Chem.* **1988**, *92*, 139–147.

(31) Seefurth, R. N.; Sharma, R. A. Investigation of the Reaction Between Liquid Lithium and Lithium Chloride-Potassium Chloride Melts. *J. Electrochem. Soc.* **1975**, *122*, 1049–1053.

(32) Sangster, J.; Pelton, A. D. Thermodynamic Calculation of Phase Diagrams of the 60 Common-Ion Ternary Systems Containing Cations Li, Na, K, Rb, Cs and Anions F, Cl, Br, I. *J. Phase Equilib.* **1991**, *12*, 511–537.

(33) von Schnering, H. G.; Schwarz, M.; Nesper, R. A Lithium Sodium Silicide  $\text{Li}_3\text{NaSi}_6$  and the formation of allo-Si. *J. Less-Common Met.* **1988**, *137*, 297–310.

(34) Grüttner, A. Über das System Lithium-Germanium und die Bildung metastabiler Germaniummodifikationen aus Li-Germaniden. Ph.D. Dissertation, Universität Stuttgart, Stuttgart, Germany, 1982.

(35) The electrodes consisted basically of  $\text{Na}_{12}\text{Ge}_{17}$  powder (about 100 mg) cold-pressed onto Mo foil, a piece of  $\alpha$ -Ge (25 mg), each wrapped into Mo gauze, and an aluminum pellet (40 mg) contacted by Mo wire; 6.85 g of the  $\text{LiI}-\text{NaI}-\text{CsI}$  electrolyte mixture in a 3.62:1:5.35 mass ratio was used.

(36) Petříček, V.; Dušek, M.; Palatinus, L. Crystallographic Computing System JANA2006: General features. *Z. Kristallogr. - Cryst. Mater.* **2014**, *229*, 345–352.

(37) Akselrud, L.; Grin, Yu. WinCSD: software package for crystallographic calculations (Version 4). *J. Appl. Crystallogr.* **2014**, *47*, 803–805.

(38) Gryko, J.; Marzke, R. F.; Lamberton, G. A., Jr.; Tritt, T. M.; Beekman, M.; Nolas, G. S. Electron structure and temperature-dependent shifts in  $^{133}\text{Cs}$  NMR spectra of the  $\text{Cs}_8\text{Ge}_{136}$  clathrate. *Phys. Rev. B: Condens. Matter Mater. Phys.* **2005**, *71*, 115208.

(39) Böhm, H. Materials for High Temperature Batteries. In *Handbook of Battery Materials*; Besenhard, J. O., Ed.; Wiley-VCH: Weinheim, Germany, 1999; pp 565–591.

(40) Beekman, M.; Kaduk, J. A.; Huang, Q.; Wong-Ng, W.; Yang, Z.; Wang, D.; Nolas, G. S. Synthesis and crystal structure of  $\text{Na}_{1-x}\text{Ge}_{3+z}$ : a novel zeolite-like framework phase in the Na–Ge system. *Chem. Commun.* **2007**, 837–839.

(41) Stefanoski, S.; Finkelstein, G. J.; Ward, M. D.; Zeng, T.; Wei, K.; Bullock, E. S.; Beavers, C. M.; Liu, H.; Nolas, G. S.; Strobel, T. A. Zintl Ions within Framework Channels: The Complex Structure and Low-Temperature Transport Properties of  $\text{Na}_4\text{Ge}_{13}$ . *Inorg. Chem.* **2018**, *57*, 2002–2012.

(42) Beekman, M.; Gryko, J.; Rubin, H. F.; Kaduk, J. A.; Wong-Ng, W.; Nolas, G. S. Synthesis and Transport Properties of Type II Clathrates. *24th International Conference on Thermoelectrics*, Clemson, SC, 2005; ICT, 2005; pp 234–237.

(43) Böhme, B. Neue Präparationswege für intermetallische Verbindungen. Ph.D. Dissertation, Technische Universität Dresden, 2010. (Published in Logos: Berlin, Germany, 2010.)

(44) Kume, T.; Ban, T.; Ohashi, F.; Jha, H. S.; Sugiyama, T.; Ogura, T.; Sasaki, S.; Nonomura, S. A thin film of a type II Ge clathrate epitaxially grown on a Ge substrate. *CrystEngComm* **2016**, *18*, 5630–5638.

(45) Hoch, C.; Simon, A.  $\text{Na}_{11}\text{Hg}_{52}$  –  $\text{Na}_{11}\text{Hg}_{52}$ : Complexity in a Polar Metal. *Angew. Chem., Int. Ed.* **2012**, *54*, 3262–3265.

(46) *Electrodeposition from Ionic Liquids*; Endres, F., MacFarlane, D., Abbott, A., Eds.; Wiley-VCH: Weinheim, Germany, 2008.

(47) van Vugt, L. K.; van Driel, A. F.; Tjerkstra, R. W.; Bechger, L.; Vos, W. L.; Vanmaekelbergh, D.; Kelly, J. J. Macroporous germanium by electrochemical deposition. *Chem. Commun.* **2002**, 2054–2055.

(48) Meng, X.; Al-Salman, R.; Zhao, J.; Borissenko, N.; Li, Y.; Endres, F. Electrodeposition of 3D Ordered Macroporous Germanium from Ionic Liquids: A Feasible Method to Make Photonic Crystals with a High Dielectric Constant. *Angew. Chem., Int. Ed.* **2009**, *48*, 2703–2707.